Mathematical modeling and numerical seismic study of smart concrete beams

M. S. Zarei[1*] , M. H. Hajmohammad[2], A. Farrokhian[2], R. Kolahchi[3]

1- Dept. of Engineering, Ayatollah Boroujerdi University, Boroujerd, Iran
2- Dept. of Mechanical Engineering, Imam Hossein University, Tehran, Iran
3- Dept. of Civil Engineering, Jasb Branch, Islamic Azad University, Jasb, Iran

* Corresponding Author: *mshzarei@abru.ac.ir*
(Received: March 2022, Accepted: June 2022)

Keywords

Mathematical modelling
Numerical solution
Seismic response
Smart concrete beam
DQ-Newmark methods
External voltage
Sinusoidal theory

Abstract

The seismic response of the smart layer is studied in this article based on mathematical modeling and numerical solution. The structure is modeled by sinusoidal shear deformation (SSDT) and the motion equations are derived by energy method and virtual work. The concrete beam is covered by a piezoelectric layer for smart control of the structure. The differential quadrature (DQ) and Newark methods are applied for numerical solution and dynamic response of the smart concrete beam under the earthquake load. The influences of boundary conditions; external voltage, and geometrical parameters of the beam are studied on the seismic response of the smart concrete beam. The results indicate that by applying an external negative voltage, the dynamic deflection of the smart concrete beam is reduced, which is important for smart control of the system while this phenomenon is converse for positive external voltage.

1. INTRODUCTION

Concrete beams are one of the important elements of the structure and hence, the dynamic analysis of this structure is essential. In addition, smart control of the concrete beam under the dynamical load is another important subject in civil engineering. In this paper, we used a piezoelectric layer for smart control of a concrete beam based on a numerical solution.

In the field of mechanical behavior and modeling of different structures, Lee and Kim [1] studied elastic analysis of two-layers smart beams by the spectral element solution method. Narayanan and Balamurugan [2] presented a numerical solution for laminated structures with smart layers as sensors and actuators. Nonlinear free vibration of nanocomposite porous beams was studied by Rafiee et al [3]. Li et al. [4] investigated the bending and vibration of smart beams by the energy method. Djojodihardjo et al. [5] studied smart control of the cantilevered smart beams by the numerical solution. Hajmohammad et al. [6] presented smart control and vibration of layerwise shells by the DQ method. Zhao et al. [7] studied vibration analysis of piezoelectric smart beams using Hamilton's principle. The mechanical response of sandwich nanocomposite plates was investigated by Mehar et al. [8]. The dynamic nonlinear response of the smart laminated nanocomposite shell was presented by Mallek et al. [9]. The vibration response of smart laminated piezoelectric beams under the thermal load was studied by Zhao et al. [10]. Hybrid responses of nanocomposite plates were studied by Pandey et al. [11] using the numerical method of the finite element. Khaje khabaz et al. [12] studied the vibration smart control of a sandwich beam on a micro-scale with piezoelectric layers. Motezaker et al. [13] studied the vibration, buckling, and bending of smart plates in the nanoscale by the numerical method of differential cubature. The seismic response of beams and columns was presented by Yang et al. [14]. Wang et al. [15]

studied the free vibration response of laminated smart beams under hygrothermal loads. Pan et al. [42] studied the dynamic response of concrete beams using experimental analysis.

For concrete structures, there are some limited works such as Zamani et al. [17]. Xiao et al. [18] studied an experimental investigation that concerns the feasibility of vibro-acoustic techniques in buried large-diameter gas pipelines for leak detection and location. A model of the correlation function of the leak noise in gas pipes was developed by Xiao et al. [19]. Xiao et al. [20] applied the acoustic method has proven to be effective for leak detection and location in gas pipelines. Meydani et al. [21] presented a Bayesian decision model for the maintenance planning of a water pipeline network. Roy et al. [22] investigated the effects of water pipe network uncertainties on the seismic vulnerability assessment of networks.

This topic is new and important in civil and mining engineering since the most important load in buildings is an earthquake and good design of the structure is essential. Hence, the dynamic response of the smart concrete beams under earthquake load is presented in this paper for the first time. The structure is modeled by SSDT and the corresponding motion equations are derived by virtual work. The numerical methods of DQ and Newmark are applied to obtain the dynamic deflection of the structure. The influences of boundary conditions; external voltage, and geometrical parameters of the beam are studied on the seismic response of the smart concrete beam.

2. FORMULATION

Fig. 1 presents a concrete beam with the smart layer under the earthquake load where the length and thickness of the beam are shown with L and h, respectively. In addition, the smart layer is subjected to the external voltage of V0.

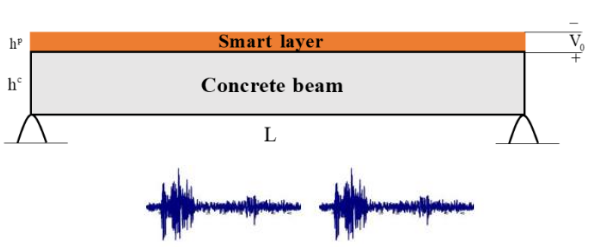

Fig. 1. Concrete beam with a smart layer under earthquake load.

Based on SSDT, the displacement field and the corresponding strain relations can be written as [23].

$$u_1(x,z,t)=u(x,t)-z\frac{\partial w(x,t)}{\partial x}+\underbrace{\left(\frac{h}{\pi}\sin\left(\frac{\pi z}{h}\right)\right)}_{f}\psi(x,t), \quad (1)$$

$$u_2(x,z,t)=0, \quad (2)$$

$$u_3(x,z,t)=w(x,t), \quad (3)$$

$$\varepsilon_{xx}=\frac{\partial u}{\partial x}-z\frac{\partial^2 w}{\partial x^2}+f\frac{\partial \psi}{\partial x}, \quad (4)$$

$$\varepsilon_{xz}=\cos\left(\frac{\pi z}{h}\right)\psi, \quad (5)$$

Where u and w are middle plane displacements. The stress relations for the concrete beam and smart layer can be written as [24]:

$$\sigma^c_{xx}=C_{11}\varepsilon_{xx}, \quad (6)$$

$$\sigma^c_{xz}=C_{55}\varepsilon_{xz}, \quad (7)$$

$$\sigma^p_{xx}=Q_{11}\varepsilon_{xx}-e_{31}E_z, \quad (8)$$

$$\sigma^p_{xz}=Q_{55}\varepsilon_{xz}-e_{15}E_x, \quad (9)$$

$$D_x=e_{15}\varepsilon_{xz}+\in_{11}E_x, \quad (10)$$

$$D_z=e_{31}\varepsilon_{xx}+\in_{33}E_z, \quad (11)$$

where Cij is elastic constant of concrete; Q_{ij}, $\in_{ij}$, and e_{ij} are elastic, dielectric, and piezoelectric coefficients of the smart layer, respectively, D_x and D_z are electrical displacements and E_k is electric which can be defined as [24]:

$$\mathrm{E_k}=-\nabla\left(-\cos\left(\frac{\pi z}{h}\right)\varphi(x,t)+\frac{2V_0 z}{h}\right). \quad (12)$$

Hamilton's principle is applied to the motion equations as follows:

$$\int_0^t\left(\delta\left(\frac{1}{2}\int_V\left(\begin{matrix}\sigma^c_{xx}\varepsilon_{xx}+\sigma^c_{xz}\varepsilon_{xz}+\sigma^p_{xx}\varepsilon_{xx}\\+\sigma^p_{xz}\varepsilon_{xz}-D_xE_x-D_zE_z\end{matrix}\right)dV\right)\right.$$
$$-\delta\left(\frac{\rho}{2}\int_v\left(\left(\frac{\partial u_1}{\partial t}\right)^2+\left(\frac{\partial u_2}{\partial t}\right)^2+\left(\frac{\partial u_3}{\partial t}\right)^2\right)dV\right) \quad (13)$$
$$\left.-\delta\left(\int_{F_{Seismic}}(ma(t))wdA\right)\right)dt=0$$

Where m and $a(t)$ are the mass and acceleration of the earth, respectively. By simplifying the above relation, the following motion equations can be derived:

$$\delta u : \frac{\partial N_x}{\partial x} = I_0 \frac{\partial^2 u}{\partial t^2}, \tag{14}$$

$$\delta w : \frac{\partial^2 M_x}{\partial x^2} + N_x^E \frac{\partial^2 w}{\partial x^2} = I_0 \frac{\partial^2 w}{\partial t^2} + \frac{24 I_2}{\pi^3} \frac{\partial^2 \psi}{\partial x \partial t} - I_2 \frac{\partial^4 w}{\partial x^2 \partial t^2} + \mathrm{F}_{Seismic}, \tag{15}$$

$$\delta \psi : \frac{\partial P_x}{\partial x} - Q_x = \frac{6 I_2}{\pi^2} \frac{\partial^2 \psi}{\partial t^2} - \frac{24 I_2}{\pi^3} \frac{\partial^2 w}{\partial x \partial t}, \tag{16}$$

$$\delta \phi : \int_{-h/2}^{h/2} \left(\frac{D_z \pi}{h} \sin\left(\frac{\pi z}{h}\right) + \cos\left(\frac{\pi z}{h}\right) \frac{\partial D_x}{\partial x} \right) dz = 0. \tag{17}$$

where N_x^E is the in-plane external load and

$$\left(N_x, M_x, P_x\right) = \int_{A^c} \left(1, z, f\right) \sigma_{xx}^c dA^c + \int_{A^p} \left(1, z, f\right) \sigma_{xx}^p dA^p, \tag{18}$$

$$Q_x = \int_{A^c} \frac{\partial f}{\partial z} \sigma_{xz}^c dA^c + \int_{A^p} \frac{\partial f}{\partial z} \sigma_{xz}^p dA^p. \tag{19}$$

By inserting Eqs. (4)-(11) into Eqs. (18) and (19), we have:

$$N_x = \left(A^p Q_{11} + A^c C_{11}\right) \frac{\partial u}{\partial x} + 2 e_{31} V_0, \tag{20}$$

$$M_x = \left(-Q_{11} I^P - C_{11} I^c\right) \frac{\partial^2 w}{\partial x^2} + \frac{24\left(-Q_{11} I^P - C_{11} I^c\right)}{\pi^3} \frac{\partial \psi}{\partial x}, \tag{21}$$

$$P_x = -\frac{24\left(-Q_{11} I^P - C_{11} I^c\right)}{\pi^3} \frac{\partial^2 w}{\partial x^2} + \frac{6 Q_{11} I \left(-Q_{11} I^P - C_{11} I^c\right)}{\pi^2} \frac{\partial \psi}{\partial x} + \frac{e_{31} h}{2} \phi, \tag{22}$$

$$Q_x = \frac{\left(Q_{55} A^p + C_{55} A^c\right)}{2} \psi - \frac{e_{15} h}{2} \frac{\partial \phi}{\partial x}, \tag{23}$$

where:

$$\left(A^j, I^j\right) = \int_{A^j} \left(1, z^2\right) dA^j \quad j = p, c, \tag{24}$$

The general boundary supports as assumed, as:

- Clamped- Clamped

$$\begin{aligned} w &= u = \frac{\partial w}{\partial x} = 0 \quad @ \quad x = 0 \\ w &= u = \frac{\partial w}{\partial x} = 0 \quad @ \quad x = L \end{aligned} \tag{25}$$

- Simply- Simply

$$\begin{aligned} w &= u = M_x = 0 \quad @ \quad x = 0 \\ w &= u = M_x = 0 \quad @ \quad x = L \end{aligned} \tag{26}$$

- Clamped-Simply

$$\begin{aligned} w &= u = \frac{\partial w}{\partial x} = 0 \quad @ \quad x = 0 \\ w &= u = M_x = 0 \quad @ \quad x = L \end{aligned} \tag{27}$$

3. NUMERICAL SOLUTION

There are a lot of numerical methods to solve the initial-and/or boundary value problems which occur in the engineering domain. Some of the common numerical methods are the finite element method (FEM), Galerkin method, finite difference method, DQM and etc. FEM and FD methods for higher-order modes require a great number of grid points. Therefore, these solution methods for all these points need more CPU time, while the DQM has several benefits that are listed below:

- DQM is a powerful method that can be used to solve numerical problems in the analysis of structural and dynamical systems.
- The accuracy and convergence of the DQM are higher than FEM.
- DQM is an accurate method for the solution of nonlinear differential equations in an approximation of the derivatives.
- This method can easily and exactly satisfy a variety of boundary conditions and require much less formulation and programming effort.
- Recently, DQM has been extended to handle irregularly shaped.

Due to the above striking merits of the DQM, in recent years the method has become increasingly popular in the numerical solution of problems in engineering and physical science. Based on the DQ method, the motion equations can be changed to algebraic equations using [24]:

$$\frac{df}{dx} \overset{x=x_i}{\rightarrow} = \sum_{j=1}^{N} C_{ij} f_j \tag{28}$$

where the weighting constants of C_{ij} and Chebyshev's polynomial roots are:

$$C_{ij}^{(1)} = \frac{L_1(x_i)}{(x_i - x_j)L_1(x_j)} \quad \text{for} \quad i \neq j, \quad i, j = 1, 2, ..., N \tag{29a}$$

$$C_{ii}^{(1)} = -\sum_{j=1, j\neq i} C_{ij}^{1} \quad \text{for} \quad i = j, \ i = 1, 2, ..., N. \tag{29b}$$

$$X_i = \frac{L}{2}\left[1 - \cos\left(\frac{i-1}{N_x - 1}\right)\pi\right] \qquad i = 1, ..., N_x \tag{30}$$

Finally, the matrix form of the motion equations is:

$$\left(\begin{bmatrix} K_{bb} & K_{bd} \\ K_{db} & K_{dd} \end{bmatrix}\begin{Bmatrix} d_b \\ d \end{Bmatrix} + \begin{bmatrix} M_{bb} & M_{bd} \\ M_{db} & M_{dd} \end{bmatrix}\begin{Bmatrix} \ddot{d}_b \\ \ddot{d}_d \end{Bmatrix}\right) = \begin{Bmatrix} 0 \\ -Ma(t) \end{Bmatrix}, \tag{31}$$

Where *[M]* and *[K]* are, respectively, the matrix of mass and stiffness, respectively; index b and *d* are boundary and domain points, respectively. The above relation based on Newmark's numerical method can be written as [25]:

$$\left[K_L + K_{NL}(d_{i+1}) + \frac{1}{\chi \Delta t^2} M\right](d_{i+1}) = \left[Q_{i+1} + M\left(\frac{1}{\chi \Delta t^2} d_i + \frac{1}{\chi \Delta t}\dot{d}_i + \left(\frac{1}{2\chi} - 1\right)\ddot{d}_i\right)\right], \tag{32}$$

Where $\gamma = 0.5$ and $\chi = 0.25$. The velocity and acceleration vectors can be found in [25]. By the above numerical method, the dynamic deflection of the structure can be obtained.

4. RESULTS AND DISCUSSION

In the results section, a concrete beam with a length of *3 m* and a thickness of *30 cm* is assumed. The elastic modulus of concrete is $E^c = 20\ GPa$ and Poisson's ratio is $\nu^c = 0.3$. For the smart layer made from Polyvinylidene fluoride (PVDF), we have elastic constants of $Q_{11} = 8\ GPa$ and $Q_{55} = 1.8\ GPa$; piezoelectric constants of $e_{31} = -0.51\ c/m^2$ and $e_{15} = -0.45\ c/m^2$ as well as the dielectric constant of $\in_{15} = 7.77e-8\ F/m$. The acceleration of the Cape Mendocino earthquake is presented in Fig. 2 for the case study.

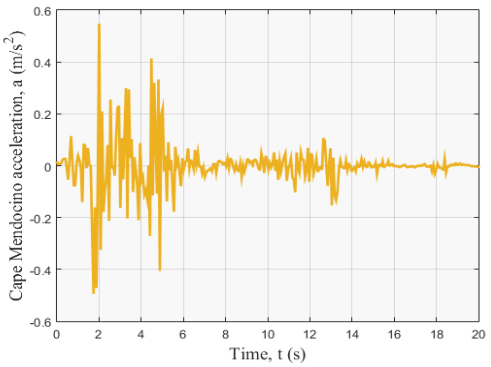

Fig. 2. Acceleration of the Cape Mendocino earthquake.

Since the model of this paper is new and a similar paper cannot be found in the literature, we computed the results with two methods of Newmark and Runge-Kutta and compared outcomes in Fig. 3.

For the exact solution, we applied the Navier method for the pipe with simply-simply boundary conditions with below dynamic deflections:

$$\begin{Bmatrix} u \\ v \\ w \end{Bmatrix} = \begin{Bmatrix} u_0 \cos\left(\frac{n\pi x}{a}\right)\sin(m\theta) \\ v_0 \sin\left(\frac{n\pi x}{a}\right)\cos(m\theta) \\ w_0 \sin\left(\frac{n\pi x}{a}\right)\sin(m\theta) \end{Bmatrix} \tag{33}$$

By substituting Eq. (33) into motion equations, we have the below final motion equation:

$$\left([K]\{d\} + [C]\{\dot{d}\} + [M]\{\ddot{d}\}\right) = \{-Ma(t)\}, \tag{34}$$

Finally, with the Newmark method, we can obtain the dynamic deflection. As can be seen, the results of the two methods match each other.

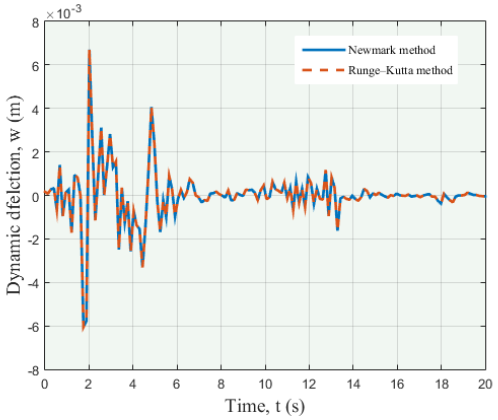

Fig. 3. Comparison of Newmark and Runge-Kutta methods.

Fig. 4 illustrates the DQ convergence on the dynamic deflection of the smart sandwich beam. It is obvious that by enhancing the number of grid

points, the maximum dynamic deflection is decreased until N=15. After N-15, the results converged and we did have not any change in the results.

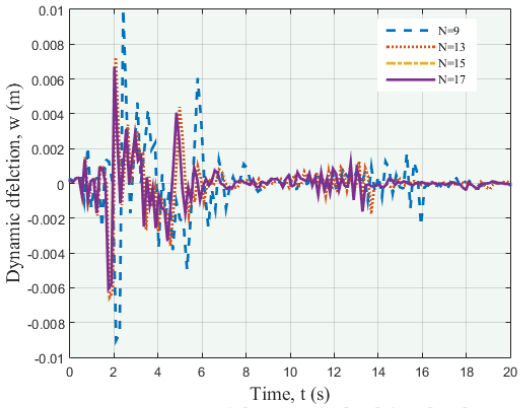

Fig. 4. Convergence of the DQ method for the dynamic deflection of the smart sandwich beam.

The external voltage effect on the dynamic deflection of the smart sandwich beam is presented in Fig. 5. It is concluded that by applying an external negative voltage to the smart layer, the dynamic deflection is reduced while this is the converse for the external positive voltage. It is reasonable since by applying external negative and positive voltages to the smart layer, a compressive and tensile load will be induced in the structure, respectively. The results of this figure are very important for the smart control of the structure.

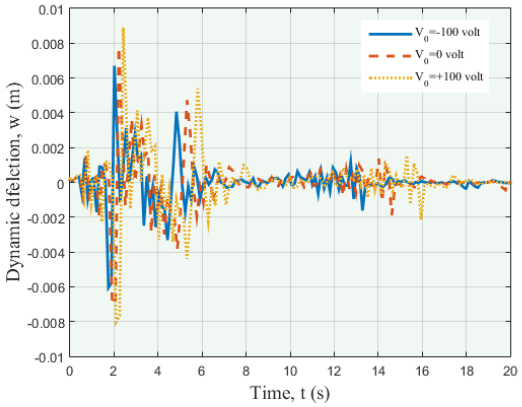

Fig. 5. The influence of external voltage on the dynamic deflection of the smart sandwich beam.

Fig. 6 demonstrates the ratio of smart to concrete thickness on the dynamic deflection of the smart sandwich beam. It is obvious that by enhancing the ratio of smart to concrete thickness, the dynamic deflection is reduced due to more stiffness in the structure.

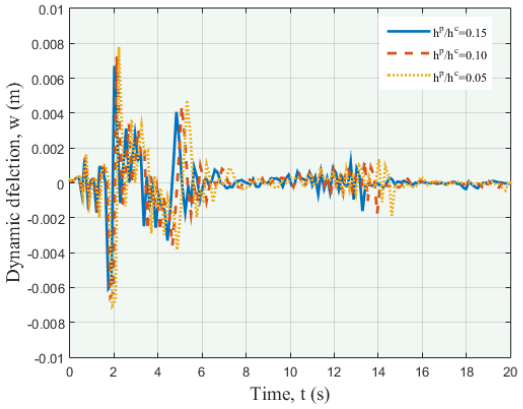

Fig. 6. The influence of the ratio of smart to concrete thickness on the dynamic displacement of the smart sandwich beam.

Fig. 7 shows the effect of various boundary conditions on the dynamic deflection of the smart sandwich beam. As it is found, the concrete beam with both ends clamped has lower dynamic deflection with respect to SS or CS concrete beam. It is because in this case, we have more bending rigidity.

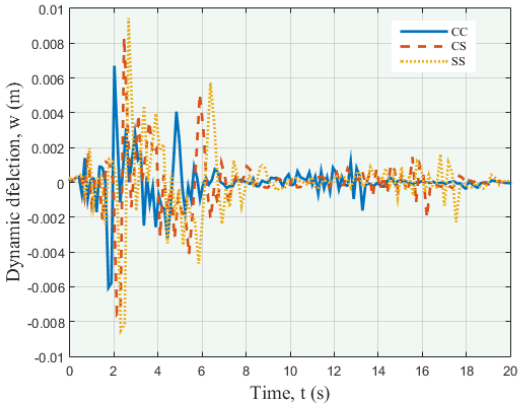

Fig. 7. The influence of boundary conditions on the dynamic displacement of the smart sandwich beam.

The effect of the beam length on the dynamic displacement is presented in Fig. 8. It can be seen that with increasing the length of the concrete beam, the dynamic deflection is increased since the stiffness of the structure is reduced.

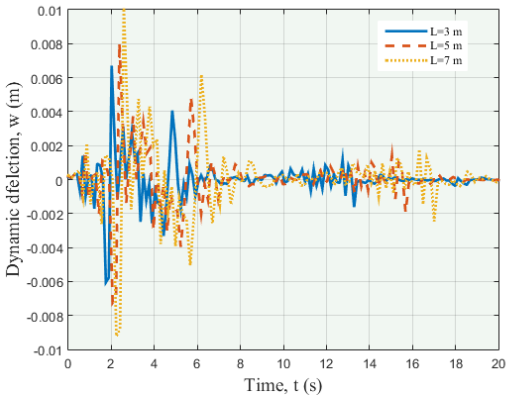

Fig. 8. The influence of the beam length on the dynamic displacement of the smart sandwich beam.

5. CONCLUSION

On the basis of mathematical modeling and numerical solution, seismic response and smart control of the concrete beam were presented in this paper. . The SSDT was applied for modeling and the corresponding motion equations were derived by the energy method. DQ and Newmark methods were used for the dynamic response of the smart sandwich concrete beam. The influences of boundary conditions; external voltage, and geometrical parameters of the beam were studied on the seismic response of the smart concrete beam. The results show that:

- It was obvious that by enhancing the number of grid points, the maximum dynamic deflection was decreased until N=15. After N-15, the results converged and we did have not any change in the results .
- Applying the negative voltage, the dynamic deflection of the structure decreased, which was very important for the smart control of the concrete structure .
- It was obvious that by enhancing the ratio of smart to concrete thickness, the dynamic deflection was reduced due to more stiffness in the structure .
- The concrete beam with both ends clamped has lower dynamic deflection with respect to SS or CS concrete beam .
- It can be seen that with increasing the length of the concrete beam, the dynamic deflection was increased.

REFERENCES

[1] Lee U, Kim J. Dynamic stability analysis and control of a composite beam with piezoelectric layers. Int J Solids Struct 2000;37:4403–17.

[2] Narayanan S, Balamurugan V. Finite element modelling of piezolaminated smart structures for active vibration control with distributed sensors and actuators. J Sound Vib 2003;262:529-62.

[3] Rafiee M, Yang J, Kitipornchai S. Large amplitude vibration of carbon nanotube reinforced functionally graded composite beams with piezoelectric layers. Compos Struct 2013;96:716–25.

[4] Li YS, Feng WJ, Cai ZY. Bending and free vibration of functionally graded piezoelectric beam based on modified strain gradient theory. Compos Struct 2014;115:41–50.

[5] Djojodihardjo H, Jafari M, Wiriadidjaja S, Ahmad, KA. Active Vibration Suppression of an elastic piezoelectric sensor and actuator fitted cantilevered beam configurations as a generic smart composite structure. J Sound Vib 2015;132:848-63.

[6] Hajmohhamad MH, Farrokhian A, Kolahchi R. Smart control and vibration of viscoelastic actuator-multiphase nanocomposite conical shells-sensor considering hygrothermal load based on layerwise. Aerosp Sci Technol 2018;78:260-70.

[7] Zhao Q, Liu Y, Wang L, Yang H, Cao D. Design method for piezoelectric cantilever beam structure under low frequency condition. Int J Pavement Res and Technol 2018;11:153-59.

[8] Mehar K, Panda SK, Patle BK. Stress, deflection, and frequency analysis of CNT reinforced graded sandwich plate under uniform and linear thermal environment: A finite element approach. Polym Compos 2018;39(10):3792-09. *https://doi.org/10.1002/pc.24409.*

[9] Mallek H, Jrad H, Wali M, Dammak F. Nonlinear dynamic analysis of piezoelectric-bonded FG-CNTR composite structures using an improved FSDT theory. Eng Comput 2019;. *https://doi.org/10.1007/s00366-019-00891-1.*

[10] Zhao X, Legaink, FGN, Zhu WD, Li YH. Coupled thermo-electro-elastic forced vibrations of piezoelectric laminated beams by means of Green's functions. Int J Mech Sci 2019;156:355-69.

[11] Pandey HK, Hirwani CK, Sharma N, Katariya PV, Panda SK. Effect of nano glass

cenosphere filler on hybrid composite eigenfrequency responses - An FEM approach and experimental verification. Adv Nano Res 2019;7(6):419-29. *http://dx.doi.org/10.12989/anr.2019.7.6.419.*

[12] Khaje Khabaz M, Eftekhari SA, Hashemian M. Toghraie D. Optimal vibration control of multi-layer micro-beams actuated by piezoelectric layer based on modified couple stress and surface stress elasticity theories. Physica A Stat. Mech Appl 2020;546:123998. *https://doi.org/10.1016/j.physa.2019.123998.*

[13] Motezaker M, Jamali M, Kolahchi R. Application of differential cubature method for nonlocal vibration, buckling and bending response of annular nanoplates integrated by piezoelectric layers based on surface-higher order nonlocal-piezoelasticity theory. Comput Appl Math 2020;369:112625. *https://doi.org/10.1016/j.cam.2019.112625.*

[14] Yang J, Guo T, Chai S. Experimental and numerical investigation on seismic behaviours of beam-column joints of precast prestressed concrete frame under given corrosion levels Structures 2020;27:1209-21.

[15] Wang L, Yang J, Li YH. Nonlinear vibration of a deploying laminated Rayleigh beam with a spinning motion in hygrothermal environment. Eng Comput 2020; *https://doi.org/10.1007/s00366-020-01035-6.*

[16] Pan HH, Wang CK, Tia M, Su, YM. Influence of water-to-cement ratio on piezoelectric properties of cement-based composites containing PZT particles. Constr Build Mater 2020; 239:117858. *https://doi.org/10.1016/j.conbuildmat.2019.117858.*

[17] Zamani Abbas, Kolahchi R, Rabani Bidgoli M. Seismic response of smart nanocomposite cylindrical shell conveying fluid flow using HDQ-Newmark methods. Comput Concrete 2017; 20:671-82.

[18] Xiao, R., Hu, Q. and Li, J. Experimental investigation on vibro-acoustic techniques to detect and locate leakages in gas pipelines, Measurement Sci. Technol., 2021; 32: 320-341.

[19] Xiao, R., Joseph, P.F., Muggleton, J.M. and Li, J. Limits for leak noise detection in gas pipes using cross correlation, J. Sound Vib., 2021; 520, 116639.

[20] Xiao, R., Hu, Q. and Li, J. Experimental Investigation on Characteristics of Leak Noise in Gas Pipeline Systems, J. Pipeline Syst. Eng. Pract. 2022;13, DOI: 10.1061/(ASCE)PS.1949-1204.0000619.

[21] Meydani, R., Giertz, T. and Leander, J. Decision with Uncertain Information: An Application for Leakage Detection in Water Pipelines", J. Pipeline Syst. Eng. Pract., 2022; 13, DOI:10.1061/(ASCE)PS.1949-1204.0000644.

[22] Roy, A., Shahandashti, M. and Rosenberger, J.M. Effects of Network Uncertainty on Seismic Vulnerability Assessment of Water Pipe Networks, J. Pipeline Syst. Eng. Pract. 2022; 13, *https://doi.org/10.1061/(ASCE)PS.1949-1204.0000652.*

[23] Thai HT, Vo TP. A nonlocal sinusoidal shear deformation beam theory with application to bending, buckling, and vibration of nanobeams. Int J Eng Sci 2012;54:58–66.

[24] Kolahchi R, Safari M, Esmailpour M. Dynamic stability analysis of temperature-dependent functionally graded CNT-reinforced visco-plates resting on orthotropic elastomeric medium. Compos Struct 2016;150:255–65.